APPLYING ASTM INTERNATIONAL C1421 TO GLASSES AND OPTICAL CERAMICS

Jonathan A. Salem
NASA Glenn Research Center
Cleveland, OH USA

Michael G. Jenkins
California State University, Fresno
Fresno, CA USA

SUMMARY

Fracture toughness is a critical structural design parameter and an excellent metric to rank structural materials. It determines fracture strength by way of the flaws, both inherent and induced, and defines the endpoint of the slow crack growth (SCG) curve. The fracture toughnesses of glasses and structural and optical ceramics as measured by several techniques is compared. When good metrology is employed, the results are very comparable with two exceptions: materials exhibiting crack growth resistance (R-curve) and those with low SCG exponents. For materials exhibiting R-curves, the result is a function of extension and can be minimized with short cracks. For materials with low SCG exponents, such as glasses, elimination of the corrosive media and/or increasing the stress intensity rate produces consistent results. A summary of values is given for optical materials and glasses.

INTRODUCTION

Fracture toughness is a critical structural design parameter and an excellent metric to rank structural materials. It determines fracture strength by way of the flaws, both inherent and induced, and defines the endpoint of the slow crack growth curve thereby representing flaw tolerance.

For design of aerospace structures, quality measurements are required for environments ranging from high vacuum and low temperature (e.g. the International Space Station) to high humidity and high temperature (e.g. a Florida launch pad near the ocean).

A number of fracture toughness definitions have been developed, particularly in the standardization literature: (1) Fracture toughness—a generic term for measures of resistance of extension of a crack (ASTM E399[1], ASTM E1823[2]); (2) Crack extension resistance at the onset of crack extension under specific operational conditions (stable or unstable) (ASTM E399); and (3) the measured stress intensity factor corresponding to the extension resistance of a stably-extending crack in a chevron-notched test specimen (ASTM C1421[3]). For engineering purposes, fracture toughness measurements generally boil down to a procedure specific value requiring a real, measurable crack within a well-defined configuration.

In this regard, because it can be difficult to produce consistent, sharp, measurable precracks for fracture testing, ASTM International introduced an excellent standard on fracture toughness measurement of ceramics in 2000[3-5]. ASTM C1421 *Standard Test Methods for Determination of the Fracture Toughness of Advanced Ceramics at Ambient Temperatures* was developed by committee C28 on Advanced Ceramics over the course of five years of effort. The method covers the determination of K_{Ipb} (single-edged pre-cracked beam or SEPB), K_{Isc} (surface crack in flexure or SCF) and K_{Ivb} (chevron-notched beam or VB), illustrated in Figure 1. All three methods produce very similar results as demonstrated in the following sections.

Prior to ASTM C1421 and its three standardized test methods, the reported fracture toughness for the same ceramic was quite variable. For example, the reported fracture toughness as measured using methods similar to those in C1421 ranged from 2.41 ± 0.14 to 3.45 ± 0.15 for Hexoloy SA (α-SiC)[6-11], a very consistently manufactured material. Indeed, when additional methods are included, the range varies from 2.41 ± 0.14 to 4.6 ± 0.13[9] MPa√m.

However, measurements using C1421 methods have much lower variability (~3%) and lower mean values as shown in Table 1 for several opaque ceramics. The methods are even capable of systematically capturing changes in the microstructure with the same material system, as shown

Table 1. Fracture toughness[2] measured per ASTM C1421.

Material	VB K_{Ivb}	SEPB K_{Ipb}	SCG K_{Isc}
α-SiC (JAS)	2.61 ± 0.05	2.58 ± 0.08	2.76 ± 0.08
α-SiC (UW)	2.62 ± 0.06	2.54 ± 0.20	2.69 ± 0.08
ADS96R	3.56 ± 0.03	3.71 ± 0.10	----
ALSIMAG 614	3.19 ± 0.06	3.09 ± 0.17	3.18 ± 0.10
NC132	4.60 ± 0.13	4.59 ± 0.12	4.55 ± 0.14
NT154	5.18 ± 0.11	5.21 ± 0.02	5.80 ± 0.23
SN260	5.19 ± 0.06	5.13 ± 0.15	----
SiAlON	----	2.45 ± 0.09	2.55 ± 0.05

in Figure 2, which compares results for SEPB and VB methods for silicon nitrides.

ASTM International C1421 was developed with an emphasis on structural heat engine ceramics as opposed to glasses and optical single crystals. Applicability of its test methods to other brittle material systems such glasses, glass-ceramics and optical materials merits further investigation because of their sensitivity to humidity combined with very low fracture toughness. Thus the questions "Is C1421 applicable to glasses and optical ceramics?" and "What issues need to be addressed?" and "What is the fracture toughness of a glass?" should be considered in applying C1421 to glasses and optical materials.

In this paper, examples of complications or interferences when testing optical materials are given, along with solutions and recommendations for changes to C1421. Finally a summary of fracture toughness values is given.

COMPLICATIONS IN FRACTURE TOUGHNESS TESTING

Interferences

All three methods standardized in ASTM C1421 have application limits when applied to brittle advanced ceramics. For the single-edge precracked beam method (SEPB), some ceramics will crush before precracking, and quality cracks cannot always be achieved. For the surface crack in flexure method (SCF), measurable cracks of acceptable geometry are not always the case. Finally, for the chevron-notched beam method (VB), stability during loading is not always achieved. In some of these cases, the interference(s) can be mitigated, but in others a different test method might be necessary for both advanced ceramics as well as glasses and optical ceramics.

Fracture toughness in the presence of stress corrosion

Subcritical crack growth due to stress corrosion occurs in many glasses and ceramics is due to bond breakage as shown in Figure 3 for a silicate structure[12]. This effect leads to rate and environment dependences of the order seen in Table 2 for alumina with a glassy boundary phase and soda-lime silicate. Values measured in air at higher rates were within 10% of dry values and thus represent reasonable engineering estimates for these two materials.

When a dry environment is used, the rate effect diminishes. This is illustrated in Figure 4 for constant stress rate testing of surface cracks in aluminum oxynitride (AlON)[13]. Thus fracture

Table 2. Average fracture toughness ± one standard deviation for ALSIMAG 614 alumina and soda-lime glass. The number of tests is given in parentheses. In air, a factor of 5x in rate leads to an 8% difference for alumina; for glass, a 12% difference occurred with a factor of 4x in rate.

K_{Ivb} *(A)* MPa√m Stroke rate	ALSIMAG 614 Alumina		
	Water	Air	Silicone oil or HP N_2
0.01 mm/min	2.64 ± 0.06 (3)	2.93 ± 0.10 (3)	3.39 ± 0.02 (2)
0.05 mm/min	2.75 ± 0.01 (4)	3.19 ± 0.07 (7)	3.37 ± 0.05 (4)
	Soda Lime Silicate Glass		
0.005 mm/min	----	0.65 ± 0.02	0.76 ± 0.01
0.01 mm/min	----	0.67 ± 0.03	----
0.02 mm/min	----	0.74 ± 0.03	0.79 ± 0.02

toughness tests in humidity are constant stress rate tests with macro-cracks. The measured values are points on the slow crack growth curve, with the unique value being that in a dry environment as shown in Figure 5. Quinn[14] has nicely shown rate effects in several glasses, with dry and fast tests converging. For estimation of slow crack growth parameters, in which the inert strength and fracture toughness are combined to estimate the initial flaw size, a dry value is recommended.

Chevron Stability

Unstable fracture in the VB decreases with increasing humidity; stress corrosion helps initiate the crack. Thus, unstable behavior can be mitigated by precracking specimens in air at a low load rate or by scratching the chevron tip, and then testing in the desired environment as shown in Figure 6. Scribing works well on softer materials, but less so on very hard materials. More aggressive machining can also be used to impart more surface damage, however, fragile specimens can be severely cracked as shown in Figure 7 for ZnS.

When precracking of SEPB specimens is difficult, precracking at a low rate, as shown in Figure 6 for the VB test method, can also be applied to a straight thru starter notch. Precracking is followed by testing in the desired environment.

Crack Length Measurements

The crack front in coarse grained materials can be difficult to delineate on the fracture surface despite being visible prior to fracture, as shown in Figures 8 and 9 for SEPB and SCF test specimens respectively. The crack front can be delineated via inks and penetrants that dry, or determined via monitoring of the specimen compliance with a clip or strain gage in the SEPB[15]. Another method is to use techniques not requiring crack length measurements like the VB and the double torsion (DT) test method.

Thin Materials

Many newer (emerging) commercial structures such as fuel cell elements and diesel particulate filters consist of thin brittle plates. The fracture toughness of such thin plates is of interest for materials assessment and life prediction. Unfortunately, none of the standard test configurations is amenable to evaluate materials in the form of thin plates. An alternative for thin sections is the DT. The DT does produce results in agreement with standard methods for materials without crack growth resistance (R-Curve) if an appropriate geometry is employed[16], as shown in Figure 10(c) for Hexoloy SA α-SiC. However, it does give elevated values for materials with R-curves such as coarse grain alumina[16], as shown in Figure 10(d).

Table 3. Fracture toughness ± one standard deviation of coarse grained spinel[18] tested per SEPB and VB test methods of ASTM C1421.

45%–65% RH		High purity N_2 (MPa√m)	
SEPB K_{Ipb}	VB K_{Ivb}	SEPB K_{Ipb}	VB K_{Ivb}
1.32 ± 0.05	1.48 ± 0.14	1.52 ± 0.07	1.58 ± 0.08

Crack Growth Resistance

Many optical ceramics possess a coarse grain structure, which produces crack growth resistance in structural ceramics such as silicon nitrides and aluminas. For ZnSe, test specimens with longer cracks tend to exhibit high fracture toughness, with standard VB specimens giving K_{Ivb} = 0.56 MPa√m while the DT gives 0.9 MPa√m as shown in Figure 11(a)[17]. Transitions from single crystal cleavage values to polycrystalline values as longer cracks are used also leads to increases in measured fracture toughness as shown in Figure 11(b). Thus, crack lengths of representative size should be used. Fortunately, the standard test configurations yield values at the lower end of the R-curve, as shown in Figures 11(a) and 12. For a coarse grained spinel[18], which also exhibits an R-curve[19], measurements via SEPB and VB methods are comparable as shown in Table 3, again demonstrating that C1421 results in consist estimates.

Data on Optical Materials

NASA, the military, and commercial enterprises use glasses and optical materials in applications ranging from sensor windows to transparent armor windows to high-grade windows for photography. Because some of these applications are fracture critical, NASA has pursued the generation of a database of standardized properties measured using full-consensus standards. Table 4 summarizes values measured via one or more standard techniques. From these data, glasses exhibit fracture toughness less than 1 MPa√m while crystalline optical ceramics exhibit values between 0.45 to 2.5 MPa√m. The effect of using standard test methods in lab air as compared to dry nitrogen produces differences ranging from a few percent to 25%, implying the need to use a dry environment.

Because of the low fracture toughness values, fracture loads are often on the order of 10 N and thus relatively small load cells might be necessary. This need can be partially mitigated by the use of shorter spans (e.g. 10/20 vs 20/40 mm), within the applicable span-to–depth ratios.

SUMMARY

Fracture toughness measurements of materials exhibiting stress corrosion are points on the SCG curve. Thus rate and environment effects occur. These effects can be minimized and consistent results obtained by using faster rates or dryer environments. The limiting value of fracture toughness occurs in a very dry environment.

ASTM International C1421 in its current form addresses many of the issue associated with testing of glasses and optical ceramics, and is generally applicable to these materials with appropriate considerations. Interferences include stress corrosion (humidity and rate), stable crack extension (VB), crack length measurement (SEPB & SCF), specimen damage (VB), material dimensions, and crack growth resistance (DT, etc.).

Review of ASTM C1421 for application to stress corrosion-sensitive materials should emphasize the use of a dry test environment and a narrower range of rates for air; the use of shorter load spans for particularly fragile materials; the use of precracking for inert (dry) testing (VB); use of compliance to measure crack length in the SEPB method; and use of the DT or buckling guides for thin SEPB specimens.

Table 4. Fracture toughness (MPa√m) of glasses and optical materials via ASTM C1421.
Data are ordered by value in dry nitrogen.

Designation	Environment		Difference
Glasses			
	Air (%RH/°F)	Dry N_2	%
Corning 0120	0.50 ± 0.02 (34/76)	0.67 ± 0.02	-25%
MOMA Pb glass[20]	0.57 ± 0.03 (30/74)	0.69 ± 0.01	-17%
Schott 8330	0.61 ± 0.04 (60/73)	0.72 ± 0.04	-15%
Schott S8061	0.64 ± 0.01 (23/73)	0.72 ± 0.02	-11%
Electro-Glass 2164	0.61 ± 0.05 (32/73)	0.74 ± 0.03	-18%
Ba-doped	0.72 ± 0.002 (23/73)	0.76 ± 0.01	-5%
Corning Silica, 7980	0.73 ± 0.04 (45/75)	0.77 ± 0.02	-5%
Soda lime silicate	0.75 ± 0.04 (35/73)	0.79 ± 0.02	-6%
Schott BK-7	0.87 ± 0.02 (24/73)	0.98 ± 0.04	-11%
Glass Ceramics			
Zerodur	0.89 ± 0.01 (45/73)	0.94 ± 0.01	-5%
Schott S8070	1.57 ± 0.03 (60/73)	1.90 ± 0.03	-17%
Crystalline Optical Ceramics			
YVO$_4$ {a}<a>	0.48 ± 0.02 (45/73)	---	
YVO$_4$ {a}<c>	0.42 ± 0.03 (45/73)	---	
ZnSe	0.55 ± 0.02 (29/73)	0.61 ± 0.03	-8%
Ge[21]	0.67 ± 0.03 (65/74)	No SCG	0%
MS ZnS	0.69 ± 0.03 (58/74)	0.74 ± 0.14	-7%
ZnS	0.74 ± 0.03 (60/72)	0.82 ± 0.02	-10%
Spinel, 220 µm g.s.[18]	1.48 ± 0.14 (60/76)	1.58 ± 0.10	-6%
Spinel, 110 µm g.s.[18]	1.66 ± 0.11 (60/76)	1.72 ± 0.25	
ALON[13]	2.09 ± 0.06 (40/70)	2.18 ± 0.10	-4%
Sapphire {a}<m>	2.06±0.21	2.31±0.11	-11%
Sapphire {r}<a>	1.96	2.47±0.15	-21%

REFERENCES

[1] ASTM E399, "Standard Test Method for Linear-Elastic Plane-Strain Fracture Toughness K_{Ic} of Metallic Materials," ASTM International V. 03.01, West Conshohocken, PA.
[2] E1823 "Standard Terminology Relating to Fatigue and Fracture Testing," ASTM International V. 03.01, West Conshohocken, PA.
[3] ASTM C1421 "Standard Test Method for the Determination of Fracture Toughness of Advanced Ceramics at Ambient Temperatures," ASTM International V. 15.01, West Conshohocken, PA.

[4] J.A. Salem, G.D. Quinn, M.G. Jenkins, "Measuring the Real Fracture Toughness of Ceramics: ASTM C1421," pp. 531-553 in Fracture Mechanics of Ceramics: Active Materials, Nanoscale Materials, Composites, Glass, and Fundamentals, R.C. Bradt et al. eds., Springer, (2005).

[5] M.G. Jenkins, J.A. Salem, G.D. Quinn, and I. Bar-on, "Development, Verification, and Implementation of a National Full-Consensus Fracture Toughness Test Method Standard for Advanced Ceramics,", pp. 49-75 in Fracture Resistance Testing of Monolithic and Composite Brittle Materials, ASTM STP 1409, J.A. Salem, G.D. Quinn and M.G. Jenkins, Eds., American Society for Testing and Materials, Philadelphia, Pennsylvania (2002).

[6] A. Ghosh, M.G. Jenkins, K.W. White, A.S. Kobayashi, and R.C. Bradt, "Elevated-Temperature Fracture Resistance of a Sintered α-Silicon Carbide," J. Am. Ceram. Soc., 72 [2] (1989) 242-247.

[7] J.A. Salem, unpublished data, NASA Lewis Research Center, Cleveland, Ohio, (1995).

[8] C.A. Tracy and G.D. Quinn, "Fracture Toughness by the Surface Crack in Flexure (SCF) Method," Cer. Eng. and Sci. Proc., 15 [5] (1994) pp. 837-845.

[9] K.D. McHenry and R.E. Tressler, "Fracture Toughness and High-Temperature Slow Crack Growth in SiC," J. Am. Ceram. Soc., 63 [3-4] (1980) pp. 152-156.

[10] M. Srinivasan and S. G. Seshadri, "Application of Single Edged Notched Beam and Indentation Techniques to Determine Fracture Toughness of Alpha Silicon Carbide," in Fracture Mechanics Methods for Ceramics Rocks, and Concrete, ASTM STP 745, Eds. S. W. Freiman, and E. Fuller, Jr., ASTM, Philadelphia, PA 1981, pp. 46-68.

[11] E.H. Kraft and R.H. Smoak, "Crack Propagation in Sintered Alpha Silicon Carbide," Presented at the Fall Meeting of the American Ceramic Society, Sept. 28, 1977, Hyannis, MA.

[12] T.A. Michalske and S.W. Freiman, "A Molecular Mechanism for Stress Corrosion in Vitreous Silica," J. Am. Ceramic Soc., Vol. 66, No. 4, pp. 284-288, April 1993.

[13] J.A. Salem, "Crack Growth Testing of an Aluminum Oxynitride (AlON) for International Space Station Kick Panes," NASA/TM—2017-219165, January 2017.

[14] G.D. Quinn and J. Swab, "Fracture Toughness of Glasses as Measured by the SCF and SEPB Methods" Ceramic Engineering and Science Proceedings, Vol. 38, No. 2, 75-88, 2017

[15] J.A. Salem and L.J. Ghosn, "Back-Face Strain for Monitoring Stable Crack Extension in Precracked Flexure Specimens," J. Am. Ceramic Soc., 93 [9] 2804–2813 (September 2010)

[16] J.A. Salem, M. Radovic, E. Lara-Curzio, G. Nelson, "Fracture Toughness of Thin Plates By The Double-Torsion Test Method,", pp. 63-73 in *Ceramic Engineering and Science Proceedings*, Vol. 27, No. 2, Mechanical Properties and Performance of Engineering Ceramics and Composites II, R. Tandon; A. Wereszczak and E. Lara-Curzio, eds (2006).

[17] J.A. Salem, "Estimation of ZnSe Crack Growth Properties for Design of the FEANICS Windows," NASA TM 213359, 2005.

[18] J.A. Salem, "Transparent Ceramics as Spacecraft Windows," Journal of the American Ceramic Society, Vol. 96, Issue 1, pages 281–289, January 2013.

[19] M.G. Jenkins, M.K. Ferber, A. Ghosh, and J. Peussa and J.A. Salem, "Chevron-Notch, Flexure Tests For Measuring the Elevated Temperature Fracture Resistance's of Structure Ceramics," pp. 159 – 177 in Chevron -Notch Test Experience: Metals and Non-Metals, ASTM STP 1172, K. R. Brown and F. I. Baratta, eds., American Society for Testing and Materials, Philadelphia, Pennsylvania, (1992).

[20] J.A. Salem, N.A. Smith and A. Ershain, "Mechanical Properties of a High Lead Glass used in the Mars Organic Molecule Analyzer, NASA/TM—2015-218847 August 2015.

[21] J.A. Salem, R. Rogers and E. Baker, "Structural Design Parameters for Germanium," Proc. of the DOD Electromagnetic Windows Symposium, May 17-19, 2016, Arlington, VA.
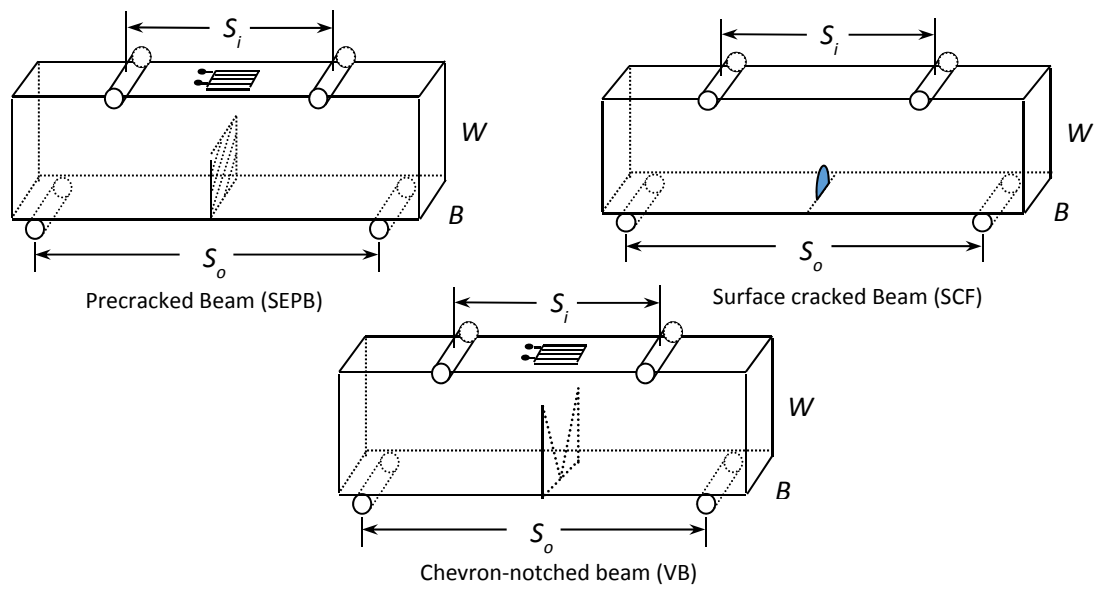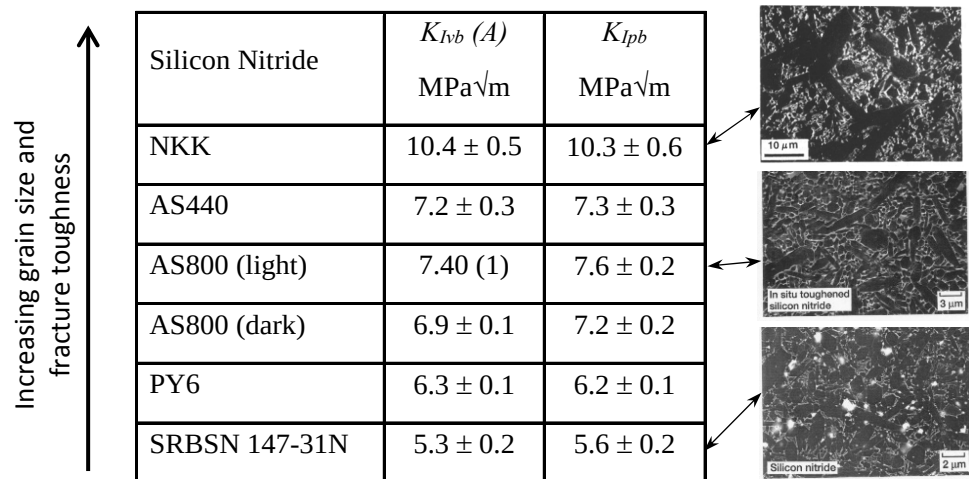
Figure 1 – ASTM C1421 test method configurations.

Silicon Nitride	K_{Ivb} (A) MPa√m	K_{Ipb} MPa√m
NKK	10.4 ± 0.5	10.3 ± 0.6
AS440	7.2 ± 0.3	7.3 ± 0.3
AS800 (light)	7.40 (1)	7.6 ± 0.2
AS800 (dark)	6.9 ± 0.1	7.2 ± 0.2
PY6	6.3 ± 0.1	6.2 ± 0.1
SRBSN 147-31N	5.3 ± 0.2	5.6 ± 0.2

Figure 2 – Fracture toughness of silicon nitrides as measured via two techniques. Increasing measured values correspond increasing grain size.
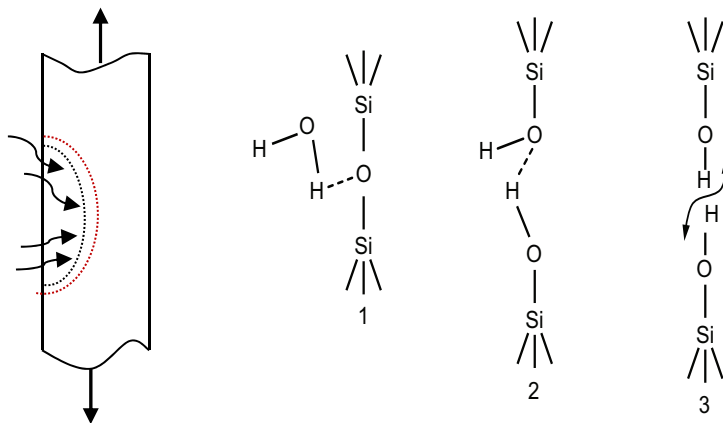
Figure 3 – Water causing bond breakage in a silicate.
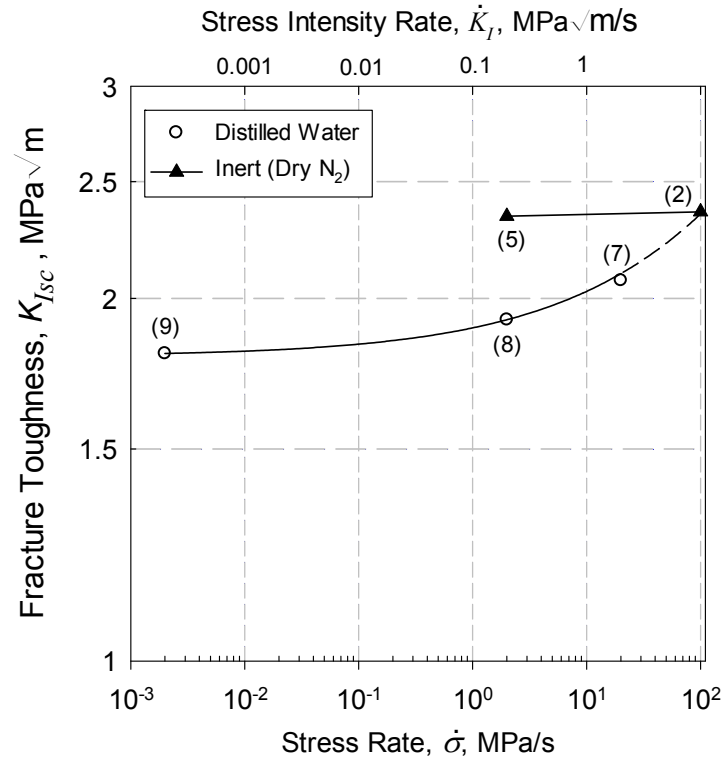
Figure 4 – Fracture toughness K_{Isc} as a function of stress rate for AlON in water and dry nitrogen.
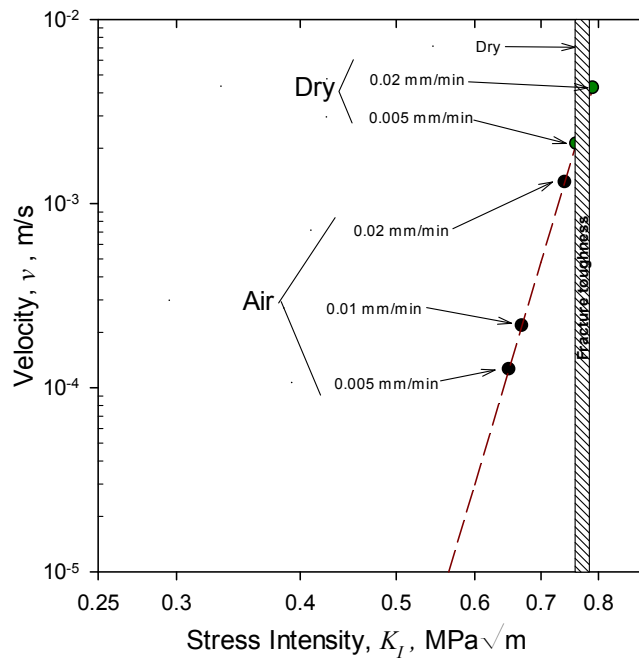
Figure 5 - Slow crack growth curve for soda-lime silicate with superimposed fracture toughness values measured at various displacement rates in air and nitrogen.
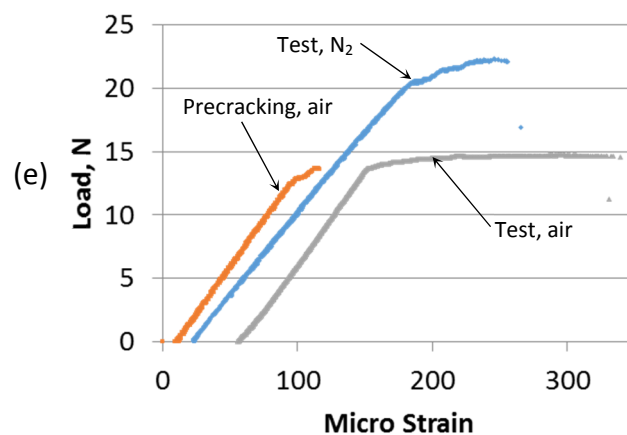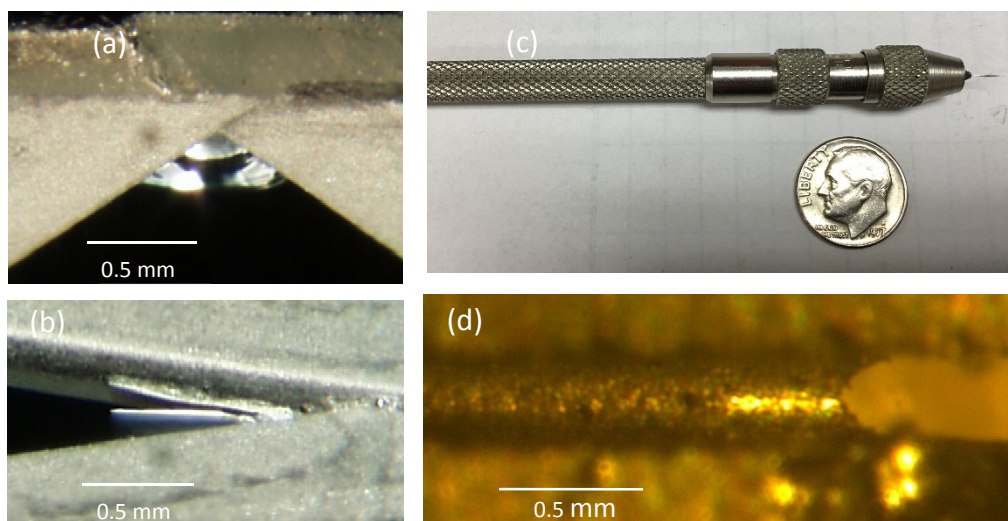
Figure 6 – (a) and (b) Precracks in a chevron notch; (c) scribe; and (d) a scratched chevron tip in ZnS; and (e) load as a function of strain.
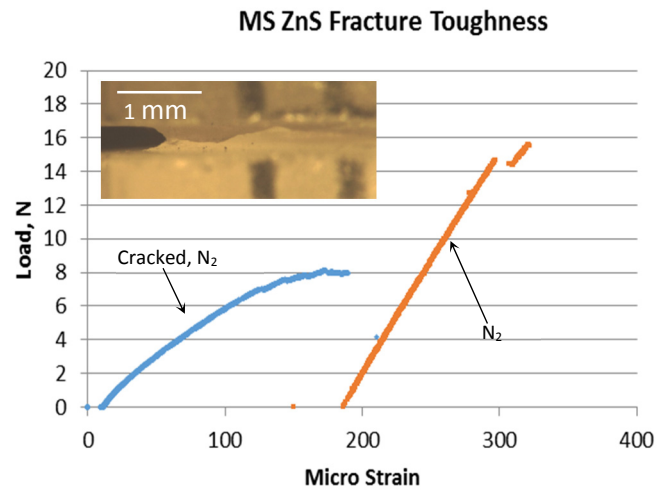
MS ZnS Fracture Toughness

Figure 7 – Effect of a severe crack on the compliance of a chevron-notched, multi-spectral ZnS specimen tested in nitrogen.
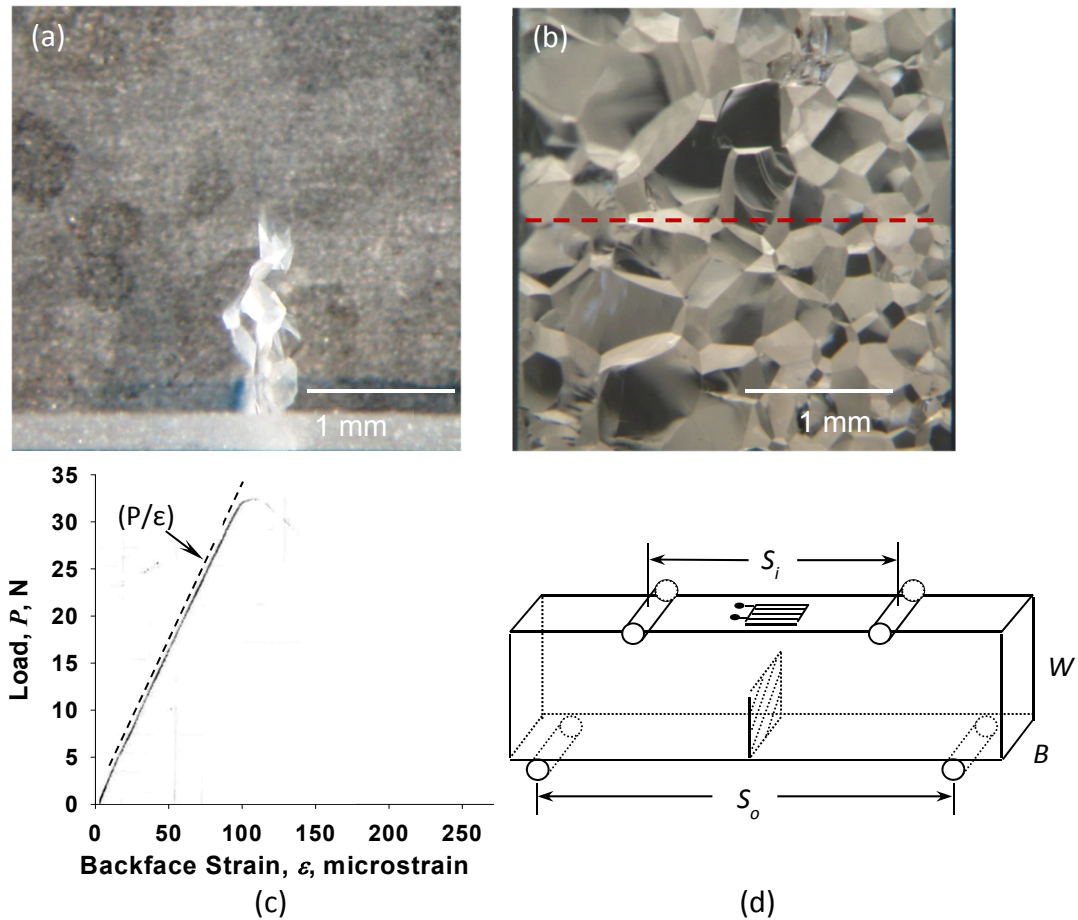
Figure 8 – (a) Precracked spinel SEPB specimen and (b) post-fracture surface. (c) Load as a function of strain for spinel SEPB specimen and (d) schematic of test specimen.
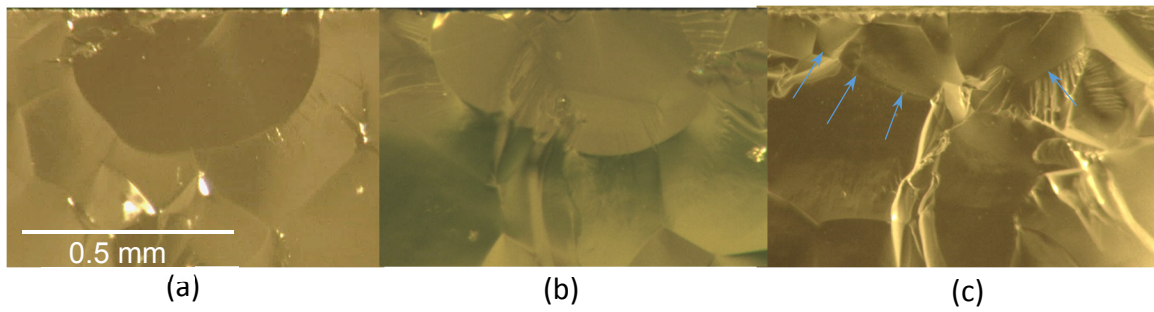
Figure 9 – Examples of SCF precracks in a coarse grained AlON: (a) well delineated; (b) poorly shaped; and (c) ill-defined.
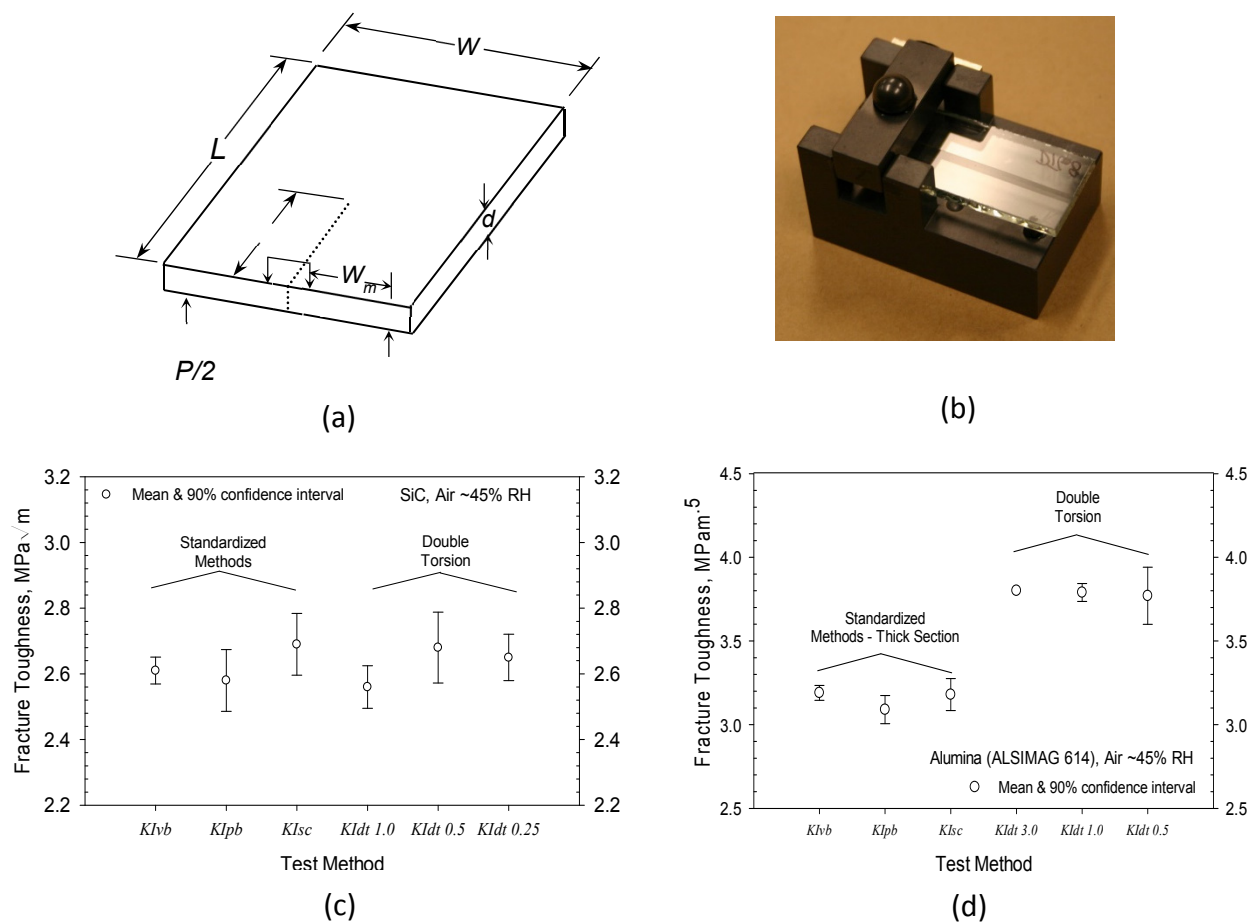

Figure 10 – (a) Schematic and (b) picture of the double torsion configuration. Comparison of DT results for various thicknesses (K_{Idt}) and standard method results for (c) silicon carbide and (d) alumina[16]. The numbers after "K_{Idt}" represent test specimen thickness in mm.
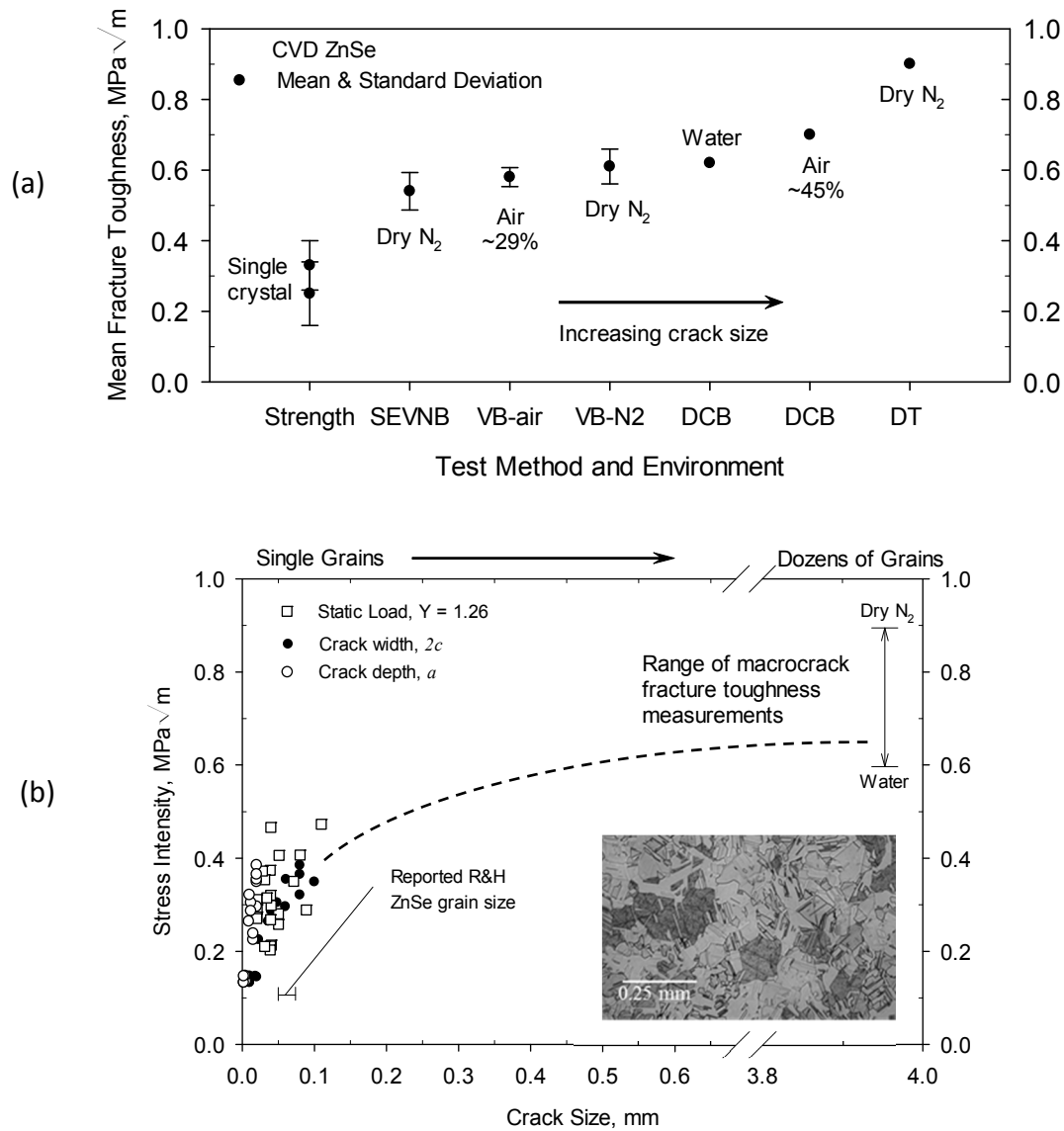
Figure 11 – (a) Fracture resistance of ZnSe as measured with specimen configurations of increasing crack size and (b) pseudo R-curve showing the transition from single crystal to polycrystalline values along with the effect of humidity.
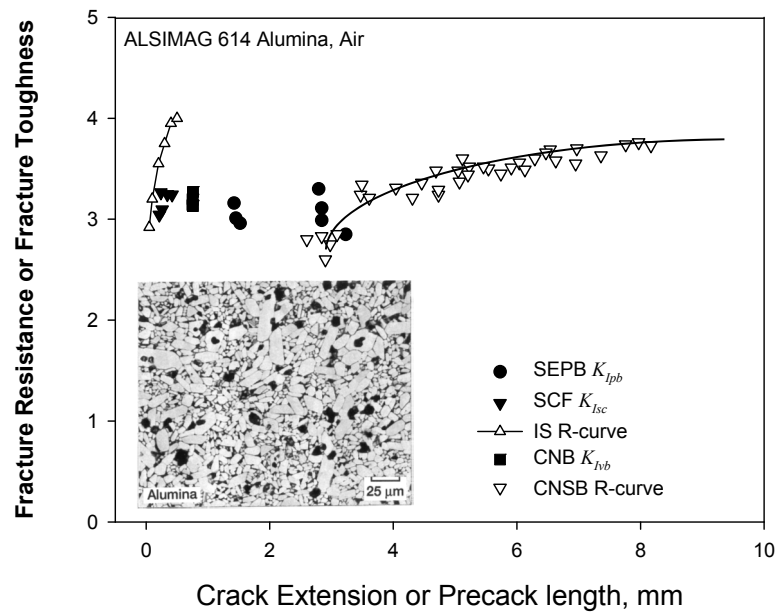
Figure 12 – Crack growth resistance of alumina along with standard fracture toughness measurements $K_{Ivb,}$ $K_{Ipb,}$ and K_{Isc}. CNSB = chevron-notch short bar; IS = indentation strength.